

Promoting long-term cycling performance of high-voltage $\text{Li}_2\text{CoPO}_4\text{F}$ by the stabilization of electrode/electrolyte interface

Xiaobiao Wu^a, Sihui Wang^a, Xiaochen Lin^a, Guiming Zhong^a, Zhengliang Gong^b, and Yong Yang^{*a,b}

^a State Key Laboratory of Physical Chemistry of Solid Surfaces, and Department of Chemistry,

College of Chemistry and Chemical Engineering, Xiamen University, Xiamen 361005, PR China.

E-mail: yyang@xmu.edu.cn

^b School of Energy Research, Xiamen University, Xiamen 361005, PR China

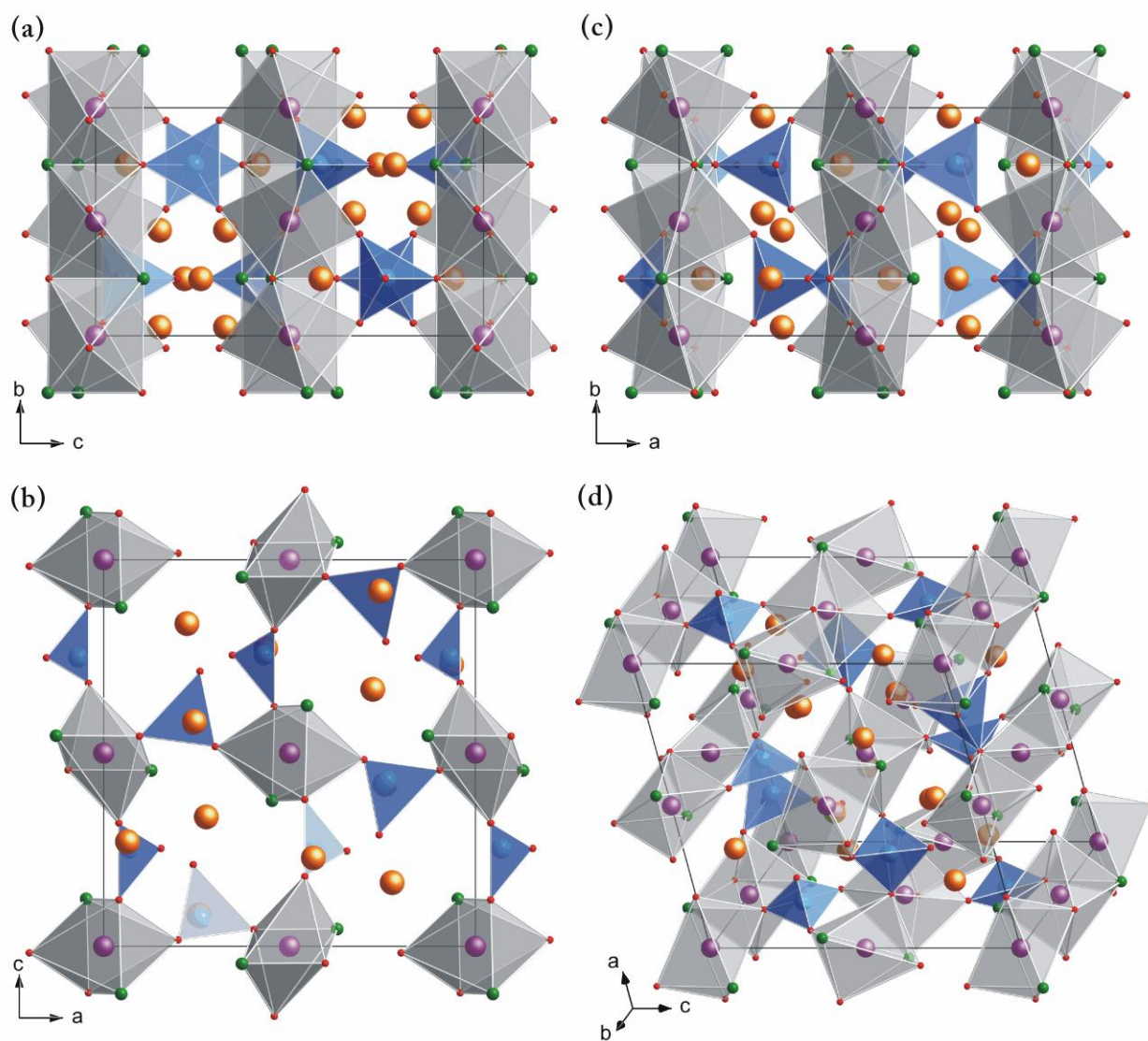


Fig. S1 Crystal structure of $\text{Li}_2\text{CoPO}_4\text{F}$: (a) view along $[100]$, (b) view along $[010]$, (c) view along $[001]$, (d) view towards (111) . The CoO_4F_2 octahedra are shown in gray and the phosphate tetrahedra are shown in blue. The lithium, cobalt, phosphorus, oxygen and fluorine atoms are shown in orange, purple, blue, red and green, respectively.

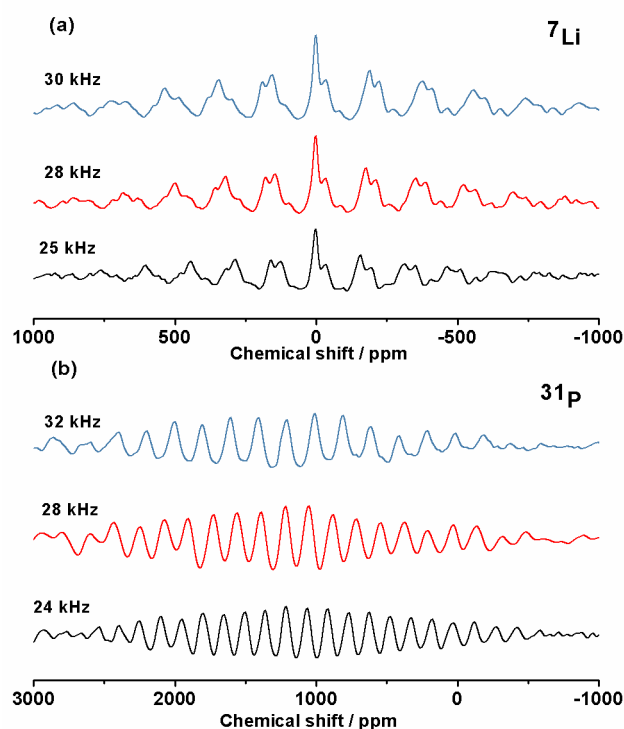


Fig. S2 ^7Li and ^{31}P MAS NMR spectra for $\text{Li}_2\text{CoPO}_4\text{F}$ at different spinning frequencies.

Figure S2 shows ^7Li and ^{31}P MAS NMR spectra for $\text{Li}_2\text{CoPO}_4\text{F}$. Different spinning frequencies were applied to identify the isotropic peaks of ^7Li and ^{31}P for $\text{Li}_2\text{CoPO}_4\text{F}$. The isotropic peaks located at 1.5 ppm, -32.6 ppm and -81.8 ppm for ^7Li , 1223.1 ppm for ^{31}P .

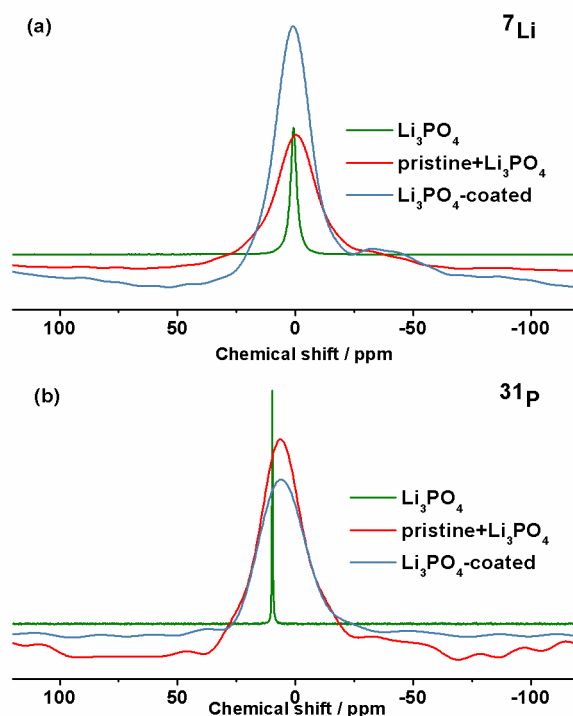


Fig. S3 ${}^7\text{Li}$ and ${}^{31}\text{P}$ MAS NMR spectra for the Li_3PO_4 , the mixture of $\text{Li}_2\text{CoPO}_4\text{F}$ and Li_3PO_4 after ball milling and Li_3PO_4 -coated $\text{Li}_2\text{CoPO}_4\text{F}$ samples.

In order to identify the chemical shifts of ${}^7\text{Li}$ and ${}^{31}\text{P}$ for Li_3PO_4 , the control experiment was carried out. A mixture of pristine $\text{Li}_2\text{CoPO}_4\text{F}$ and Li_3PO_4 was ball milled at 500 rpm for 10 h. Figure S3 shows the ${}^7\text{Li}$ and ${}^{31}\text{P}$ NMR spectra for the Li_3PO_4 , the mixture of $\text{Li}_2\text{CoPO}_4\text{F}$ and Li_3PO_4 after ball milling and the Li_3PO_4 -coated $\text{Li}_2\text{CoPO}_4\text{F}$ samples. It can be seen that the chemical shifts of ${}^7\text{Li}$ for the three samples all locate at 1.5 ppm. However, the chemical shift of ${}^{31}\text{P}$ for the Li_3PO_4 locates at 10.0 ppm, the chemical shifts for the mixture of $\text{Li}_2\text{CoPO}_4\text{F}$ and Li_3PO_4 after ball milling and Li_3PO_4 -coated $\text{Li}_2\text{CoPO}_4\text{F}$ both locate at 6.0 ppm. It is speculated that the delocalized electron of carbon and $\text{Li}_2\text{CoPO}_4\text{F}$ makes the chemical shift move upfield. Therefore, according to the control experiment, we can make a conclusion that ${}^7\text{Li}$ (1.5 ppm) and ${}^{31}\text{P}$ (6.0 ppm) are assigned to Li_3PO_4 .

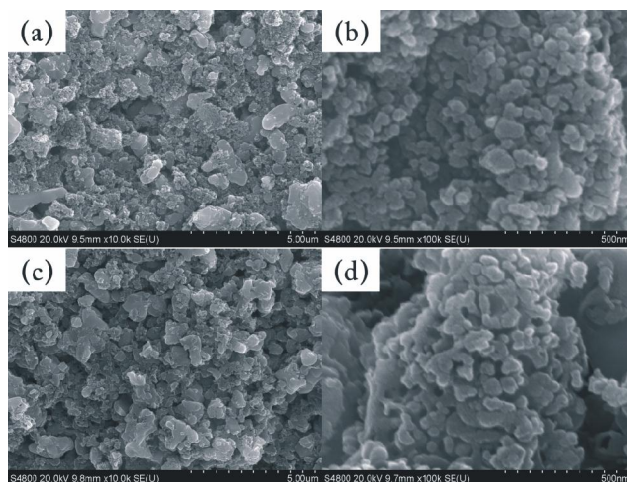


Fig. S4 SEM images of the (a, b) pristine and (c, d) Li_3PO_4 -coated $\text{Li}_2\text{CoPO}_4\text{F}$.

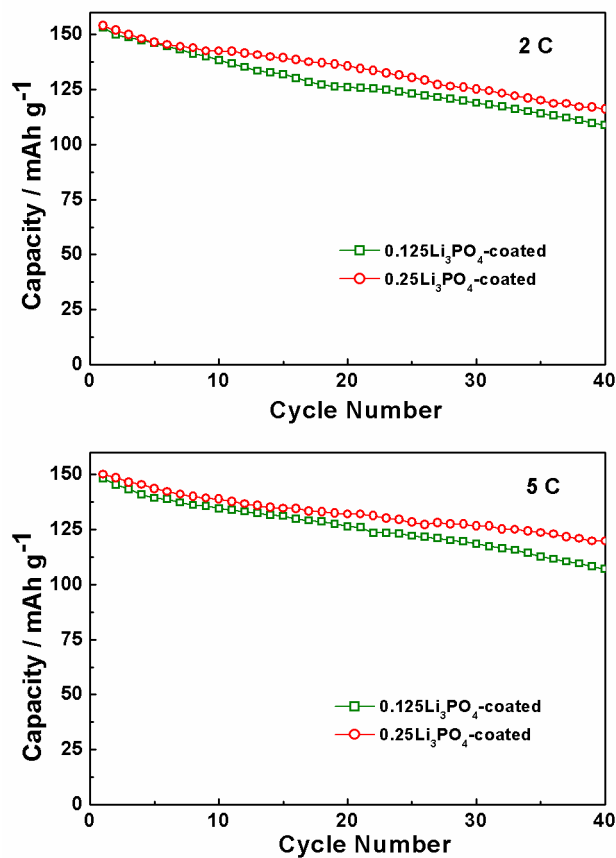


Fig. S5 Cycling performances of the 0.125 Li_3PO_4 -coated and 0.25 Li_3PO_4 -coated $\text{Li}_2\text{CoPO}_4\text{F}$ samples at 2 C and 5 C. The mole ratio of $\text{Li}_2\text{CoPO}_4\text{F}$ to Li_3PO_4 is 8:1 (marked as 0.125 Li_3PO_4 -coated) and 4:1 (marked as 0.25 Li_3PO_4 -coated).

Figure S2 shows the cycling performances of the 0.125 Li_3PO_4 -coated and 0.25 Li_3PO_4 -coated $\text{Li}_2\text{CoPO}_4\text{F}$ samples. It can be clearly seen that 0.25 Li_3PO_4 -coated $\text{Li}_2\text{CoPO}_4\text{F}$ sample shows superior cycling performance than 0.125 Li_3PO_4 -coated $\text{Li}_2\text{CoPO}_4\text{F}$ sample.

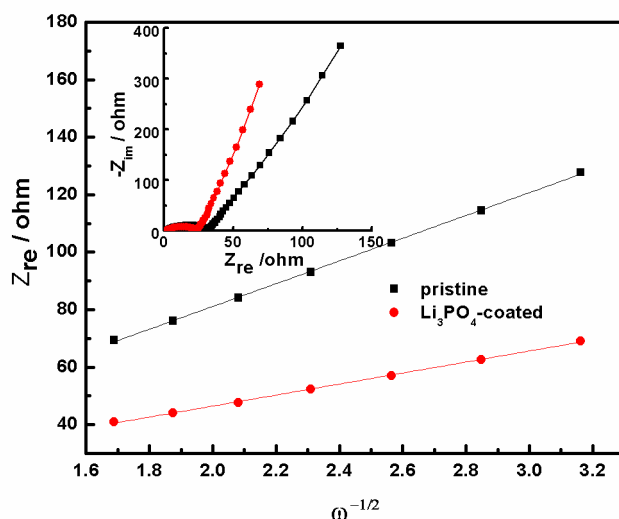


Fig. S6 The relationship between Z_{re} and $\omega^{-1/2}$ at low frequencies. The inset is the Nyquist plots of the pristine and the Li_3PO_4 -coated $\text{Li}_2\text{CoPO}_4\text{F}$. The data were collected at the open circuit voltage. The frequency range is from 100 kHz to 0.1 Hz.

The lithium ion diffusion coefficient is evaluated according to the equation¹:

$$D = 0.5R^2T^2/A^2n^4F^4C^2\sigma^2$$

Where R is the gas constant, T is the absolute temperature, A is the electrode area, n is the number of electrons per molecule during reaction, F is the Faraday constant, C is the concentration of lithium ion, σ is Warburg factor which obeys relationship with Z_{re} :

$$Z_{re} = R_e + R_{ct} + \sigma\omega^{-1/2}$$

Figure S6 shows the relationship between Z_{re} and $\omega^{-1/2}$. The slope σ is obtained from the linear fitting of Z_{re} versus $\omega^{-1/2}$. Therefore, $D_{coated} / D_{pristine} = (\sigma_{pristine} / \sigma_{coated})^2 = 4.3$.

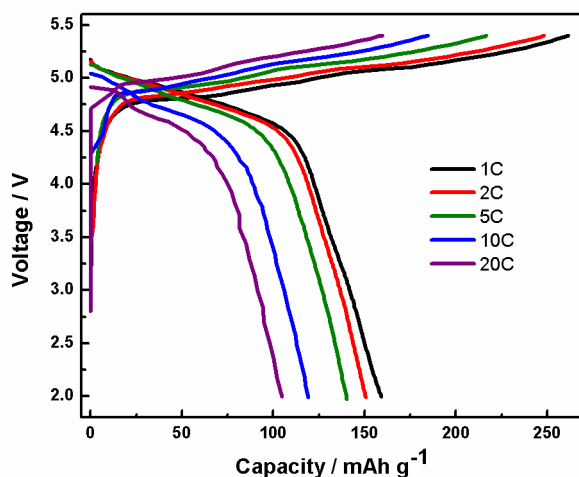


Fig. S7 The first charge/discharge profiles of the 0.5 Li_3PO_4 -coated $\text{Li}_2\text{CoPO}_4\text{F}$ at various rates.

The mole ratio of $\text{Li}_2\text{CoPO}_4\text{F}$ to Li_3PO_4 is 2:1 (marked as 0.5 Li_3PO_4 -coated).

Figure S7 shows the first first charge/discharge profiles of the 0.5 Li_3PO_4 -coated $\text{Li}_2\text{CoPO}_4\text{F}$ at various rates. It can be seen that 0.5 Li_3PO_4 -coated sample exhibits a discharge capacity of 105 mAh g^{-1} at 20 C current rate, which is only 66.0% of that at 1 C.

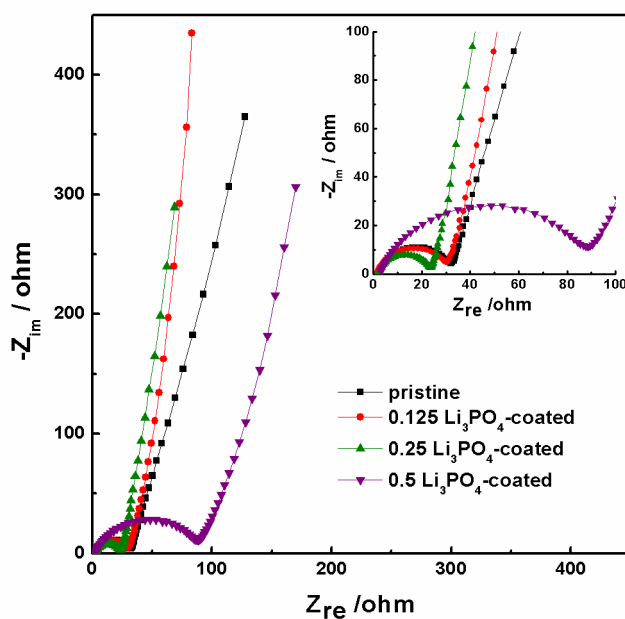


Fig. S8 Nyquist plots of the pristine and the Li_3PO_4 -coated $\text{Li}_2\text{CoPO}_4\text{F}$ at the open circuit voltage.

The frequency range is from 100 kHz to 0.1 Hz.

Figure S8 shows the Nyquist plots of the pristine and the Li_3PO_4 -coated $\text{Li}_2\text{CoPO}_4\text{F}$ at the open circuit voltage. The high-medium frequency semicircle is related to the charge transfer resistance (R_{ct}), and the low frequency slope region represents lithium ion diffusion in bulk material. It can be clearly seen that the charge transfer resistance of the 0.5 Li_3PO_4 -coated $\text{Li}_2\text{CoPO}_4\text{F}$ is much larger than that of the other three samples. The excess amount of Li_3PO_4 with poor electronic conductivity coating on the surface of active material goes against the charge transfer, and then affects rate performance.

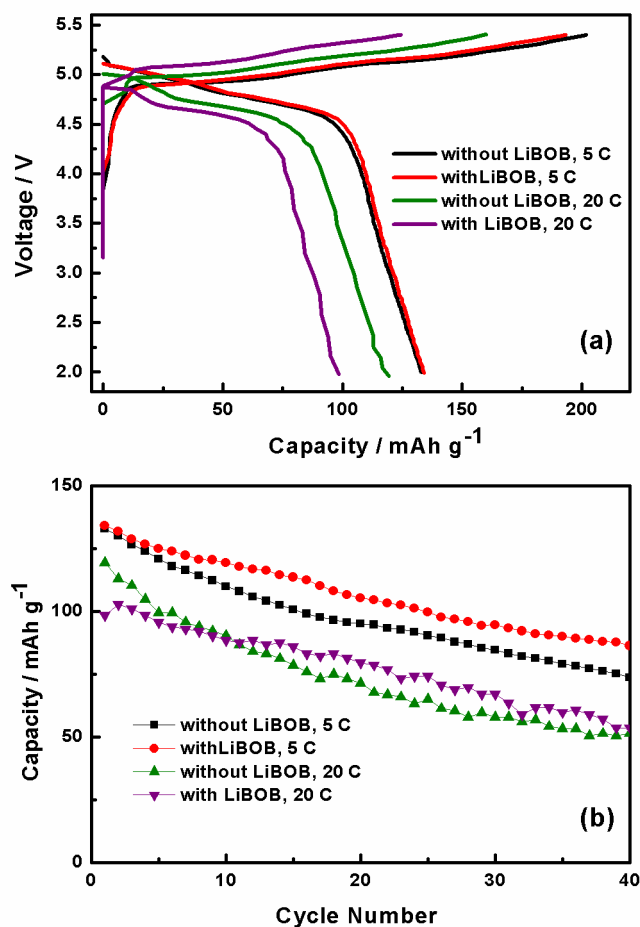


Fig. S9 The first charge/discharge profiles (a) and cycling performances (b) of the pristine $\text{Li}_2\text{CoPO}_4\text{F}$ in electrolyte with and without LiBOB additive at 5 C and 20 C current rates.

Figure S9 shows the first charge/discharge profiles and cycling performances of the pristine $\text{Li}_2\text{CoPO}_4\text{F}$ in electrolyte with and without LiBOB additive. $\text{Li}_2\text{CoPO}_4\text{F}$ in electrolyte with LiBOB additive shows similar charge/discharge profile compared to that in electrolyte without LiBOB additive at 5 C. However, the discharge capacity and working voltage decrease at 20 C for the case in electrolyte with LiBOB additive. It can be seen that LiBOB electrolyte additive can improve the cycling performances at both 5 C and 20 C current rates. These results are similar to that of the Li_3PO_4 -coated $\text{Li}_2\text{CoPO}_4\text{F}$ in electrolyte with and without LiBOB additive.

Table S1 The initial coulombic efficiencies for the $\text{Li}_2\text{CoPO}_4\text{F}$ samples at various rates.

sample	1C	2C	5C	10C	20C
pristine	53.8	58.8	65.9	72.4	74.6
Li_3PO_4 -coated	62.4	64.7	71.4	73.6	76.8
Li_3PO_4 -coated+LiBOB	66.7	70.3	74.8	74.5	75.5

Table S1 summarizes the initial coulombic efficiencies for the $\text{Li}_2\text{CoPO}_4\text{F}$ samples at various rates.

It can be seen that the surface modification and electrolyte additive can improve the initial coulombic efficiency compared with the pristine sample at various rates, especially at low current rate. It is believed that surface modification and film-forming electrolyte additive can reduce the contact area between active material and electrolyte, and then reduce the decomposition of electrolyte.

1. H. Liu, C. Li, H. P. Zhang, L. J. Fu, Y. P. Wu and H. Q. Wu, *J. Power Sources*, 2006, **159**, 717-720.